Control System with State Feedback and NN based Load Torque Feedforward for PMSM with LC Filter Fed by 3-Level NPC Inverter

L. M. Grzesiak[1] and T. Tarczewski[2]
[1]Institute of Control and Industrial Electronics,Warsaw University of Technology, Koszykowa 75, Warsaw, Poland
[2]Institute of Physics, Faculty of Physics, Astronomy and Informatics, Nicolaus Copernicus University, Grudziadzka 5, Torun, Poland

Keywords: Artificial Neural Network, Load Torque Feedforward, State Feedback Controller, 3-Level Neutral Point Clamped Inverter, LC Filter, Permanent Magnet Synchronous Motor, Disturbance Observer.

Abstract: This paper presents designing process of the control system with discrete state feedback and neural network based load torque feedforward for permanent magnet synchronous motor fed by true sine wave 3-level neutral point clamped inverter with an output LC filter. Our main objective is to reduce the effect of load torque changes and to improve dynamic behaviour of the motor during load changing. The full state feedback algorithm has been chosen to control the angular velocity of the motor and to provide true sine wave of the input motor voltages. It was found that gains of the controller and feedforward path are non-stationary and depends on the angular velocity. In such a case linearization and decoupling process of the motor with LC filter is not needed. Simulation results (at the level of 3kW) illustrate the proposed approach.

1 INTRODUCTION

Artificial neural networks (ANN) have been playing an important role in a motion control systems. Thanks to the universal approximation property, ANNs are successfully used for: friction modeling and compensation (Huang and Tan, 2012), deadzone function estimation and compensation (Selmic and Lewis, 2000) as well as adaptive control (Pajchrowski and Zawirski, 2012).

The control performance of permanent magnet synchronous motor (PMSM) is influenced by an external load. This performance can be improved with the help of the feedforward compensation (Iwasaki et al., 2012). Although, load torque is non-measurable variable in a typical motion system, it can be estimated with the help of the disturbance observer (Mun-Soo et al., 2001). Proper feedforward compensation requires suitable formula depends on control algorithm used.

Electromagnetic torque ripple of PMSM can be reduced when 3-level Neutral Point Clamped (NPC) true sine wave inverter with an output LC filter is used (Tarczewski and Grzesiak, 2012). Non-linear, non-stationary model of such a system causes, that the state feedback control is an attractive control method (Pawlikowski and Grzesiak, 2007).

In this paper control system with discrete state feedback controller for PMSM fed by true sine 3-level NPC inverter is presented. In order to reduce the effect of load torque changes and to improve the dynamic behaviour of PMSM during load variations, NN based non-stationary feedforward load torque path is introduced into control system.

A mathematical formula how to calculate an appropriate non-stationary gain values for a load torque feedforward path is depicted. Observed load torque is used as an input signal for the feedforward path. The discrete full state feedback controller with an internal input models is designed in order to control the angular velocity of the PMSM with respect to zero *d*-axis component of the current space vector and to provide true sine wave of the input motor voltages.

2 MATHEMATICAL MODEL OF AN ELECTROMECHANICAL SYSTEM

Considered control system consists of: discrete state feedback controller with neural network feedforward path, 3-level NPC inverter with an output LC filter,

Grzesiak L. and Tarczewski T..
Control System with State Feedback and NN based Load Torque Feedforward for PMSM with LC Filter Fed by 3-Level NPC Inverter.
DOI: 10.5220/0004484002590267
In *Proceedings of the 10th International Conference on Informatics in Control, Automation and Robotics* (ICINCO-2013), pages 259-267
ISBN: 978-989-8565-70-9

observer and PMSM. Schematic diagram of proposed control system was shown in figure 1.

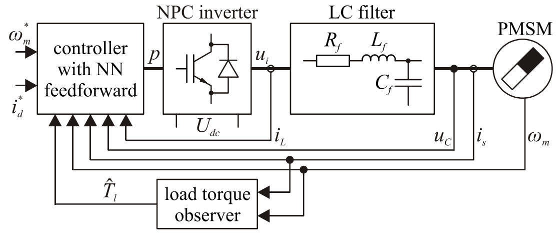

Figure 1: Proposed control system.

2.1 Model of PMSM

In order to create mathematical model of PMSM, following assumptions are made (Pillay and Krishnan, 1988), (Zawirski, 2005): eddy current and hysteresis losses are negligible, saturation is neglected, the back *emf* is sinusoidal, magnetic symmetry occurs in the circuit. In an orthogonal *d-q* coordinate system that rotates at electrical velocity ω_k of the rotor, the expression of the voltage and flux equation takes the following form (Pillay and Krishnan, 1988), (Zawirski, 2005):

$$u_{Cd} = R_s i_{sd} + \frac{\mathrm{d}\psi_d}{\mathrm{d}t} - p\omega_m \psi_q \tag{1}$$

$$u_{Cq} = R_s i_{sq} + \frac{\mathrm{d}\psi_q}{\mathrm{d}t} + p\omega_m \psi_d \tag{2}$$

$$\psi_d = L_s i_{sd} + \psi_f \tag{3}$$

$$\psi_q = L_s i_{sq} \tag{4}$$

where: u_{Cd}, u_{Cq}, i_{sd}, i_{sq}, ψ_d, ψ_q are space vector components of voltages, currents and fluxes in d and q axis, R_s is resistance of the stator, L_s is inductance of the stator, ψ_f is permanent magnetic flux linkage, p is the number of pole pairs, ω_m is rotor angular velocity.

Cross couplings between d and q axis as well as the product of an angular velocity and fluxes causes, that voltage equations (1)-(2) are non-linear.

For a PMSM with a surface mounted magnets, the electromagnetic torque is proportional to the quadrature current and it can be expressed as follows (Pillay and Krishnan, 1988), (Zawirski, 2005):

$$T_e = \frac{3}{2} p \psi_f i_{sq} = K_t i_{sq} \tag{5}$$

where K_t is motor torque constant.

Finally, to complete mathematical model of the PMSM, the following equation of mechanical motion have been added (Pillay and Krishnan, 1988), (Zawirski, 2005):

$$\frac{\mathrm{d}\omega_m}{\mathrm{d}t} = \frac{1}{J_m}\left(T_e - B_m\omega_m - T_l\right) \tag{6}$$

where: J_m is motor moment of inertia, T_l is load torque, B_m is viscous friction.

2.2 Model of Reactance Filter

Similarly to model of PMSM presented above, model of an output LC filter is described in an orthogonal *d-q* coordinate system. The expression of voltage and current equation takes the following form (Pawlikowski and Grzesiak, 2007):

$$u_{id} = R_f i_{Ld} + L_f \frac{\mathrm{d}i_{Ld}}{\mathrm{d}t} - L_f \omega_k i_{Lq} + u_{Cd} \tag{7}$$

$$u_{iq} = R_f i_{Lq} + L_f \frac{\mathrm{d}i_{Lq}}{\mathrm{d}t} + L_f \omega_k i_{Ld} + u_{Cq} \tag{8}$$

$$i_{Cd} = C_f \frac{\mathrm{d}u_{Cd}}{\mathrm{d}t} - C_f \omega_k u_{Cq} \tag{9}$$

$$i_{Cq} = C_f \frac{\mathrm{d}u_{Cq}}{\mathrm{d}t} + C_f \omega_k u_{Cd} \tag{10}$$

$$i_{Ld} = i_{Cd} + i_{sd} \tag{11}$$

$$i_{Lq} = i_{Cq} + i_{sq} \tag{12}$$

where: u_{id}, u_{iq}, i_{Ld}, i_{Lq} are space vector components of filter input voltages and currents, i_{Cd}, i_{Cq} are space vector components of currents in filter capacitance, R_f is filter resistance, L_f is filter inductance, C_f is filter capacitance.

2.3 Model of Inverter

Static model of the 3-level NPC inverter can be used if inverter operates in a linear range, the switching frequency is much higher than the electrical time constant of PMSM and if dead time of IGBTs can be ignored. Model of the inverter can be described as follows (Grzesiak and Tarczewski, 2013):

$$\begin{bmatrix} u_{id} \\ u_{iq} \end{bmatrix} = K_p \begin{bmatrix} u_{pd} \\ u_{pq} \end{bmatrix} \tag{13}$$

where: u_{pd}, u_{pq} are space vector components of inverter control voltages, K_p is gain coefficient of inverter. Presented in (Grzesiak and Tarczewski, 2013) simulation as well as experimental test results show, that described model of the inverter does not introduce any significant error.

3 DISCRETE STATE FEEDBACK CONTROLLER

Non-linear terms in equations (1)-(2) as well as in equations (7)-(10) cause that the state feedback control is an attractive approach to control described in a previous section electromechanical system.

3.1 State-space Representation of the System

In order to design state feedback controller, model of electromechanical system (1)-(13) should be rewritten in a form of the state equation:

$$\frac{d\boldsymbol{x}}{dt} = \boldsymbol{A}(\omega_k)\boldsymbol{x} + \boldsymbol{B}\boldsymbol{u} + \boldsymbol{E}d \tag{14}$$

where:

$$\boldsymbol{A}(\omega_k) = \begin{bmatrix} -a_1 & a_2 & -a_3 & 0 & 0 & 0 & 0 \\ -a_2 & -a_1 & 0 & -a_3 & 0 & 0 & 0 \\ a_4 & 0 & 0 & a_2 & -a_4 & 0 & 0 \\ 0 & a_4 & -a_2 & 0 & 0 & -a_4 & 0 \\ 0 & 0 & a_5 & 0 & -a_6 & a_2 & 0 \\ 0 & 0 & 0 & a_5 & -a_2 & -a_6 & -a_7 \\ 0 & 0 & 0 & 0 & 0 & a_8 & -a_9 \end{bmatrix},$$

$$\boldsymbol{x}^{\mathrm{T}} = [i_{Ld} \;\; i_{Lq} \;\; u_{Cd} \;\; u_{Cq} \;\; i_{sd} \;\; i_{sq} \;\; \omega_m],$$

$$\boldsymbol{B}^{\mathrm{T}} = \begin{bmatrix} \frac{K_p}{L_f} & 0 & 0 & 0 & 0 & 0 & 0 \\ 0 & \frac{K_p}{L_f} & 0 & 0 & 0 & 0 & 0 \end{bmatrix}, \boldsymbol{u} = \begin{bmatrix} u_{pd} \\ u_{pq} \end{bmatrix},$$

$$\boldsymbol{E}^{\mathrm{T}} = \begin{bmatrix} 0 & 0 & 0 & 0 & 0 & 0 & -\frac{1}{J_m} \end{bmatrix}, d = T_l,$$

$$a_1 = \frac{R_f}{L_f}, \quad a_2 = p\omega_m = \omega_k, \quad a_3 = \frac{1}{L_f},$$

$$a_4 = \frac{1}{C_f}, \quad a_5 = \frac{1}{L_s}, \quad a_6 = \frac{R_s}{L_s},$$

$$a_7 = \frac{p\psi_f}{L_s}, \quad a_8 = \frac{K_t}{J_m}, \quad a_9 = \frac{B_m}{J_m}$$

3.2 An Internal Input Model

In the proposed control algorithm steady state error of the angular velocity is caused by step variations of the reference velocity and load torque. It could be eliminated by introducing an internal model of the reference input (Grzesiak and Tarczewski, 2013). Control strategy with zero d-axis component of the current space vector is the most popular in PMSM (Zawirski, 2005). An internal model of the reference direct current has been added to ensure control strategy described above.

An augmented state equation, after introduction the internal input model and assumption, that external load torque T_l is omitted, takes the following form:

$$\frac{d\boldsymbol{x}_i}{dt} = \boldsymbol{A}_i(\omega_k)\boldsymbol{x}_i + \boldsymbol{B}_i\boldsymbol{u} + \boldsymbol{F}_i\boldsymbol{r}_i \tag{15}$$

where:

$$\boldsymbol{A}_i(\omega_k) = \begin{bmatrix} -a_1 & a_2 & -a_3 & 0 & 0 & 0 & 0 & 0 & 0 \\ -a_2 & -a_1 & 0 & -a_3 & 0 & 0 & 0 & 0 & 0 \\ a_4 & 0 & 0 & a_2 & -a_4 & 0 & 0 & 0 & 0 \\ 0 & a_4 & -a_2 & 0 & 0 & 0 & -a_4 & 0 & 0 \\ 0 & 0 & a_5 & 0 & -a_6 & 0 & a_2 & 0 & 0 \\ 0 & 0 & 0 & 0 & 1 & 0 & 0 & 0 & 0 \\ 0 & 0 & 0 & a_5 & -a_2 & 0 & -a_6 & -a_7 & 0 \\ 0 & 0 & 0 & 0 & 0 & 0 & a_8 & -a_9 & 0 \\ 0 & 0 & 0 & 0 & 0 & 0 & 0 & 1 & 0 \end{bmatrix},$$

$$\boldsymbol{x}_i^{\mathrm{T}} = [i_{Ld} \;\; i_{Lq} \;\; u_{Cd} \;\; u_{Cq} \;\; i_{sd} \;\; e_i \;\; i_{sq} \;\; \omega_m \;\; e_\omega],$$

$$\boldsymbol{B}_i^{\mathrm{T}} = \begin{bmatrix} \frac{K_p}{L_f} & 0 & 0 & 0 & 0 & 0 & 0 & 0 & 0 \\ 0 & \frac{K_p}{L_f} & 0 & 0 & 0 & 0 & 0 & 0 & 0 \end{bmatrix}, \boldsymbol{r}_i = \begin{bmatrix} i_{sd}^* \\ \omega_m^* \end{bmatrix},$$

$$\boldsymbol{F}_i^{\mathrm{T}} = \begin{bmatrix} 0 & 0 & 0 & 0 & 0 & -1 & 0 & 0 & 0 \\ 0 & 0 & 0 & 0 & 0 & 0 & 0 & 0 & -1 \end{bmatrix}$$

New state variable e_i introduced in an augmented state equation (15) corresponds to the integral of the direct current:

$$e_i(t) = \int_0^t [i_{sd}(\tau) - i_{sd}^*(\tau)]d\tau \tag{16}$$

where i^*_{sd} is the reference value of the direct current.

Similarly, state variable e_ω corresponds to the integral of the angular velocity error:

$$e_\omega(t) = \int_0^t [\omega_m(\tau) - \omega_m^*(\tau)]d\tau \tag{17}$$

where ω^*_m is the reference value of the angular velocity.

3.3 Non-stationary Discrete Controller

The control law for system described by an augmented state equation (15) can be computed from the following formula:

$$\begin{aligned} \boldsymbol{u}(t) &= -\boldsymbol{K}(\omega_k)\boldsymbol{x}_i(t) = -\boldsymbol{K}_x(\omega_k)\boldsymbol{x}(t) - \\ &- \boldsymbol{K}_{ei}(\omega_k)e_i(t) - \boldsymbol{K}_{e\omega}(\omega_k)e_\omega(t) \end{aligned} \tag{18}$$

where: $\boldsymbol{K}(\omega_k)$, $\boldsymbol{K}_x(\omega_k)$, $\boldsymbol{K}_{ei}(\omega_k)$, $\boldsymbol{K}_{e\omega}(\omega_k)$ are non-stationary gain matrices of the state feedback controller.

In order to design discrete state feedback controller suitable to implement in a DSP system, the control law presented above must be rewritten in a discrete form:

$$\begin{aligned} \boldsymbol{u}(n) &= -\boldsymbol{K}(\omega_k)\boldsymbol{x_i}(n) = -\boldsymbol{K}_x(\omega_k)\boldsymbol{x}(n) - \\ &- \boldsymbol{K}_{ei}(\omega_k)e_i(n) - \boldsymbol{K}_{e\omega}(\omega_k)e_\omega(n) \end{aligned} \tag{19}$$

where n is an index of the discrete sampling time.

By using the backward Euler integration algorithm, discrete form of the state variables e_i and e_ω were obtained:

$$e_i(n) = e_i(n-1) + T_s[i_{sd}(n) - i_{sd}^*(n)] \tag{20}$$

$$e_\omega(n) = e_\omega(n-1) + T_s[\omega_m(n) - \omega_m^*(n)] \tag{21}$$

where T_s is the sampling interval.

The discrete linear-quadratic optimization method (Tewari, 2002) was used to calculate gain coefficients of the state feedback controller at the operating points defined by the actual value of the angular velocity $\omega_k \in$ [-942; 942] rad/s. The Matlab Control System Toolbox has been used to calculate appropriate matrices.

In order to compute non-stationary gain values of the controller, the following penalty matrices has been assigned:

$$\begin{aligned} \boldsymbol{R}_i &= \mathrm{diag}([r_{i1} \quad r_{i2}]), \\ \boldsymbol{Q}_i &= \mathrm{diag}([q_{i1}\ q_{i2}\ q_{i3}\ q_{i4}\ q_{i5}\ q_{i6}\ q_{i7}\ q_{i8}\ q_{i9}]) \end{aligned} \tag{22}$$

where: $r_{i1} = r_{i2} = 3\times10^{-1}$, $q_{i1} = q_{i2} = q_{i3} = q_{i4} = 1\times10^{-5}$, $q_{i5} = 5{,}7\times10^{1}$, $q_{i6} = 1\times10^{7}$, $q_{i7} = 7{,}6\times10^{-1}$, $q_{i8} = 1\times10^{-2}$, $q_{i9} = 1{,}64\times10^{2}$.

Values of the gain matrices depicted above were selected manually in order to: provide zero steady state angular velocity error for step angular velocity reference change as well as load torque step variations, achieve twice the rated current of PMSM (i_{sn} = 5,8 A) during the step change of the reference angular velocity from 0 rad/s to 70π rad/s with the rated load torque (T_{ln} = 8,8 Nm). The assumptions presented above determine the maximum dynamics of the designed control system.

Matlab's *polyfit* and *polyval* commands were used to determine the mathematical functions that approximate dependencies between the controller's gain and the angular velocity.

Based on the simulation test results it was found that: coefficients $k_{d2}(\omega_k)$, $k_{q1}(\omega_k)$, $k_{q3}(\omega_k)$, $k_{q5}(\omega_k)$ and $k_{q6}(\omega_k)$ have the negligible impact of the control process and can be replaced by zeros; coefficients $k_{d1}(\omega_k)$, $k_{d3}(\omega_k)$, $k_{d5}(\omega_k)$, $k_{d6}(\omega_k)$, $k_{q2}(\omega_k)$, $k_{q4}(\omega_k)$, $k_{q7}(\omega_k)$, $k_{q8}(\omega_k)$ and $k_{q9}(\omega_k)$ can be replaced by constant values (independent of the angular velocity). Constant gain coefficients were computed by using *mean* function implemented in the Matlab environment. Coefficients $k_{d4}(\omega_k)$, $k_{d7}(\omega_k)$, $k_{d8}(\omega_k)$, $k_{d9}(\omega_k)$ should be implemented as the following linear functions:

$$k_{d4}(\omega_k) = 7{,}29\times10^{-7}\,\omega_k \tag{23}$$

$$k_{d8}(\omega_k) = -7{,}28\times10^{-6}\,\omega_k \tag{24}$$

$$k_{d7}(\omega_k) = 5{,}51\times10^{-5}\,\omega_k \tag{25}$$

$$k_{d9}(\omega_k) = -6{,}81\times10^{-4}\,\omega_k \tag{26}$$

Finally, gain coefficients of the discrete state feedback controller computed for the system with parameters given in table 1 and for penalty matrices (22) are as follows:

$$\boldsymbol{K}_x^{\mathrm{T}}(\omega_k) = \begin{bmatrix} 0{,}13 & 0 \\ 0 & 0{,}1 \\ 0{,}0077 & 0 \\ k_{d4}(\omega_k) & 0{,}004 \\ 0{,}62 & 0 \\ k_{d7}(\omega_k) & 0{,}31 \\ k_{d8}(\omega_k) & 0{,}053 \end{bmatrix}, \tag{27}$$

$$\boldsymbol{K}_{\boldsymbol{e}_i}(\omega_k) = \begin{bmatrix} 298{,}76 \\ 0 \end{bmatrix},\ \boldsymbol{K}_{\boldsymbol{e}_\omega}(\omega_k) = \begin{bmatrix} k_{d9}(\omega_k) \\ 5{,}71 \end{bmatrix} \tag{28}$$

Table 1: The basic parameters of the system.

Parameter	Value	Unit
R_f	3×10^{-2}	Ω
L_f	2×10^{-3}	H
C_f	6×10^{-6}	F
R_s	1,05	Ω
L_s	$9{,}5\times10^{-3}$	H
K_t	1,635	Nm/A
J_m	$6{,}2\times10^{-4}$	kgm^2
B_m	$1{,}4\times10^{-3}$	Nms/rad
K_p	291	
p	3	

4 FEEDFORWARD LOAD TORQUE COMPENSATION

Dynamic properties of the discrete state feedback controller can be improved by using the disturbance signals (Tewari, 2002). In the designed control system, load torque can be used for a feedforward compensation.

4.1 Feedforward Computation

In order to introduce feedforward path, residual model of state equation (14) should be considered (Lee et al., 1994), (Pawlikowski and Grzesiak, 2007):

$$\frac{\mathrm{d}\tilde{\boldsymbol{x}}}{\mathrm{d}t} = \boldsymbol{A}(\omega_k)\tilde{\boldsymbol{x}} + \boldsymbol{B}\tilde{\boldsymbol{u}} \tag{29}$$

where:

$$\tilde{\boldsymbol{x}} = \boldsymbol{x} - \boldsymbol{x}_{ss},\ \ \tilde{\boldsymbol{u}} = \boldsymbol{u} - \boldsymbol{u}_{ss} \tag{30}$$

are deviations from the steady state.

It can be seen, that presented above residual model is non-stationary due to the presence of ω_k in the state matrix. It was assumed that disturbance d remains constant for deviations from steady state, so it is not present in residual model (29).

The control law for the non-stationary residual model can be formulated as follows:

$$\boldsymbol{u} = -\boldsymbol{K}_x(\omega_k)\boldsymbol{x} + [\boldsymbol{K}_x(\omega_k)\ \ \boldsymbol{I}]\begin{bmatrix}\boldsymbol{x}_{ss}\\ \boldsymbol{u}_{ss}\end{bmatrix} \tag{31}$$

where $\boldsymbol{I}$ is an identity matrix with an appropriate dimension. The column vector from the right side of the control law (31) can be computed from the following form of the state equation in steady state:

$$\begin{bmatrix}\boldsymbol{x}_{ss}\\ \boldsymbol{u}_{ss}\end{bmatrix} = -\boldsymbol{G}(\omega_k)^{-1}\boldsymbol{E}d \tag{32}$$

where:

$$\boldsymbol{G}(\omega_k) = [\boldsymbol{A}(\omega_k)\ \ \boldsymbol{B}] \tag{33}$$

After substituting of (32) into (31), the control law can be rearranged as follows:

$$\boldsymbol{u} = -\boldsymbol{K}_x(\omega_k)\boldsymbol{x} - [\boldsymbol{K}_x(\omega_k)\ \ \boldsymbol{I}]\boldsymbol{G}(\omega_k)^{-1}\boldsymbol{E}d \tag{34}$$

Denoting the second component of the equation (34) as:

$$\boldsymbol{K}_d(\omega_k) = [\boldsymbol{K}_x(\omega_k)\ \ \boldsymbol{I}]\boldsymbol{G}(\omega_k)^{-1}\boldsymbol{E} \tag{35}$$

one can write the control law with the feedforward path:

$$\boldsymbol{u} = -\boldsymbol{K}_x(\omega_k)\boldsymbol{x} - \boldsymbol{K}_d(\omega_k)d \tag{36}$$

Finally, the discrete form of the control law with an internal input model of the reference signals and with the feedforward path takes the following form:

$$\begin{aligned}\boldsymbol{u}(n) = &-\boldsymbol{K}_x(\omega_k)\boldsymbol{x}(n) - \boldsymbol{K}_{ei}(\omega_k)e_i(n) - \\ &-\boldsymbol{K}_{e\omega}(\omega_k)e_\omega(n) - \boldsymbol{K}_d(\omega_k)d(n)\end{aligned} \tag{37}$$

After evaluating equation (35), it was found that the relationships between the angular velocity ω_k and feedforward gain coefficients: $\boldsymbol{K}_d^{\mathrm{T}}(\omega_k) = [k_{d1}(\omega_k)\ k_{d2}(\omega_k)]$ are nonlinear (figure 2).

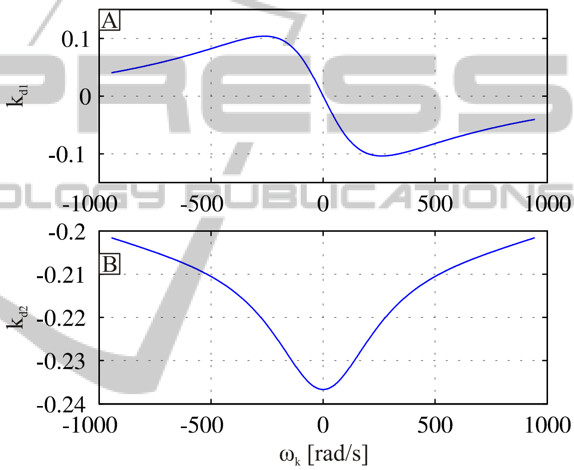

Figure 2: Values of the feedforward coefficients.

4.2 Neural Network Approximation

Since artificial neural networks have an inherent capability of learning and approximating nonlinear functions (Huang and Tan, 2012), it is attractive to apply them to approximate nonlinear dependencies presented in figure 2.

It was found that feedforward coefficients can be successfully approximated with the help of the feedforward backpropagation artificial neural network. For a neural network with 7 neurons in the first layer and 2 neurons in the output layer, satisfactory level of approximation (mean square error less than 1×10^{-7}) was achieved after 417 epochs. Schematic diagram of the designed and trained in a Matlab environment neural network approximator is presented in figure 3.

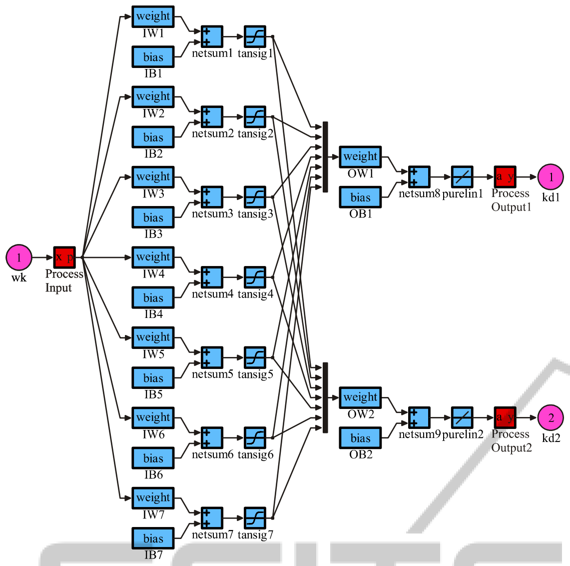

Figure 3: Neural network approximator.

5 LOAD TORQUE OBSERVER

In order to design the control system with a feedforward load torque compensation, a non-measured load torque should be estimated with the help of the observer. The discrete state equation that describes the dynamics of the system takes the following form (Mun-Soo et al., 2001):

$$\Delta \boldsymbol{x_o}(n) = \boldsymbol{A_o}\boldsymbol{x_o}(n) + \boldsymbol{B_o}u_o(n) \tag{38}$$

$$y_o(n) = \boldsymbol{C_o}\boldsymbol{x_o}(n) \tag{39}$$

where:

$$\Delta \boldsymbol{x_o}(n) = \frac{\boldsymbol{x_o}(n) - \boldsymbol{x_o}(n-1)}{T_s}, \quad \boldsymbol{B_o} = \begin{bmatrix} \frac{K_t}{J_m} \\ 0 \end{bmatrix},$$

$$\boldsymbol{x_o}(n) = \begin{bmatrix} \omega_m(n) \\ T_l(n) \end{bmatrix}, \quad \boldsymbol{A_o} = \begin{bmatrix} -\frac{B_m}{J_m} & -\frac{1}{J_m} \\ 0 & 0 \end{bmatrix}, \tag{40}$$

$$u_o(n) = i_{sq}(n), \quad \boldsymbol{C_o} = [1 \ \ 0]$$

For system (38)-(40) the following equation of the discrete load torque observer can be formulated (Luenberger, 1971):

$$\Delta \hat{\boldsymbol{x}}_{\boldsymbol{o}}(n) = \boldsymbol{A_o}\hat{\boldsymbol{x}}_{\boldsymbol{o}}(n) + \boldsymbol{B_o}u_o(n) + \boldsymbol{L}[y_o(n) - \boldsymbol{C_o}\hat{\boldsymbol{x}}_{\boldsymbol{o}}(n)] \tag{41}$$

where:

$$\hat{\boldsymbol{x}}_{\boldsymbol{o}}(n) = \begin{bmatrix} \hat{\omega}_m(n) \\ \hat{T}_l(n) \end{bmatrix}, \quad L = \begin{bmatrix} l_1 \\ l_2 \end{bmatrix} \tag{42}$$

An observable values are depicted in $\hat{\boldsymbol{x}}_{\boldsymbol{o}}$ while $\boldsymbol{L}$ is a gain matrix of the designed observer. A schematic diagram of implemented in Simulink discrete load torque observer is shown in figure 4.

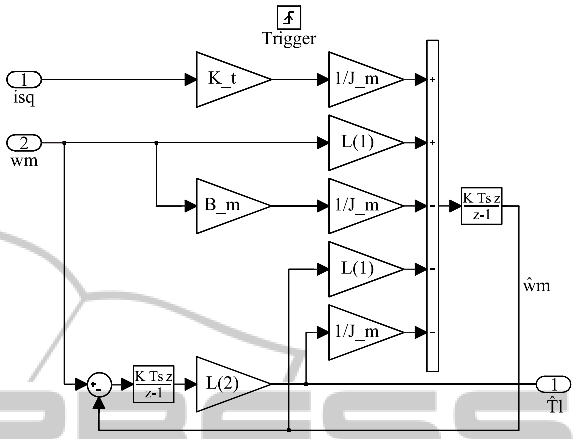

Figure 4: Block diagram of the load torque observer.

The goal of the designed load torque observer is to provide an estimate $\hat{\boldsymbol{x}}_{\boldsymbol{o}}$ so that $\hat{\boldsymbol{x}}_{\boldsymbol{o}} \to \boldsymbol{x_o}$ for $t \to \infty$. Because system (41) is fully observable, we can find $\boldsymbol{L}$ matrix so that the tracking error is asymptotically stable. Therefore, the observer design process is reduced to finding the gain matrix $\boldsymbol{L}$ so that the roots of the system (41) characteristic equation lie in the left half-plane. Gain matrix of the load torque observer was determined with the help of Matlab's *place* formula. For the pole locations:

$$o_{1/2} = -3\times 10^3 \pm 1\times 10^3 i \tag{43}$$

that guarantee the proper dynamics of the observer, values of the gain matrix $\boldsymbol{L}$ are as follows:

$$l_1 = 6\times 10^3, \quad l_2 = -6{,}2\times 10^3 \tag{44}$$

6 CONTROL SYSTEM WITH DISCRETE STATE FEEDBACK CONTROLLER AND LOAD TORQUE FEEDFORWARD

The proposed control system was tested in the Matlab/Simulink environment with the help of the Plecs blockset. The results obtained for control system with neural network based load torque feedforward path were compared with the results achieved for the state feedback based control system without feedforward.

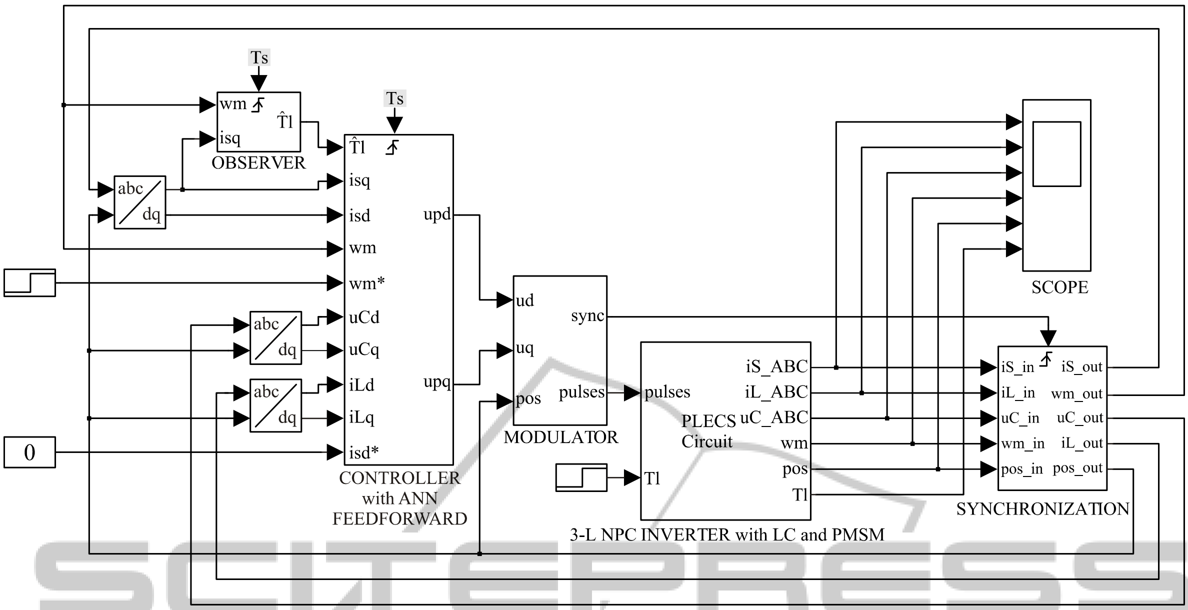

Figure 5: Schematic diagram of the designed control system.

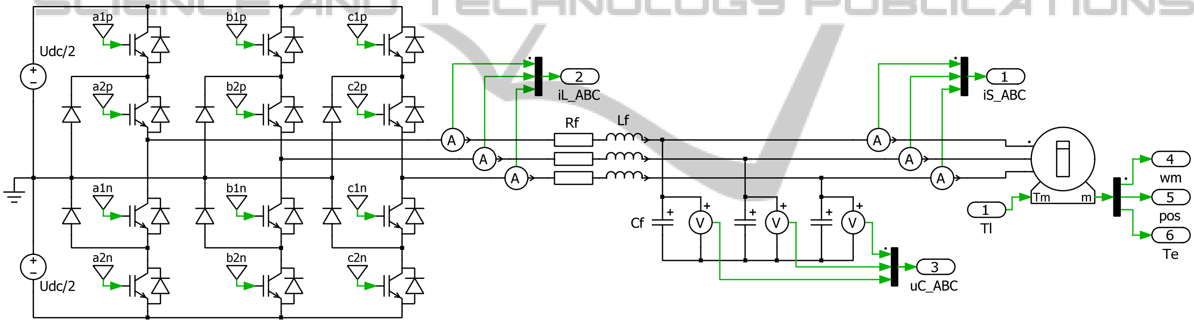

Figure 6: Schematic diagram of the PMSM with 3-level NPC inverter and LC filter.

6.1 Model of the proposed Control System

Schematic diagram of the designed control system was presented in figure 5.

Described in previous sections discrete state feedback controller as well as load torque observer were implemented in triggered subsystems in order to ensure proper generation of discrete control and estimate signals respectively. The sampling interval was set to T_s = 100 μs (the switching frequency is equal to f_s = 10 kHz).

In order to realize measurements in a midpoint of the PWM pulse length, triggered synchronization block was used.

Shown in figure 6 model of PMSM with 3-level NPC inverter as well as LC filter was implemented in the Plecs software.

Carrier-based sinusoidal PWM with level shifted triangular carriers modulation method was used to control switches in the 3-level NPC inverter (Rodriguez et al., 2010).

For the proper operation of the designed control system the resonance frequency of the LC filter (f_r = 1453 Hz) was set to be almost ten times higher than the rated frequency of the motor (f_m = 150 Hz) and almost seven times lower than the switching frequency (Steinke, 1999).

6.2 Simulation Test Results

Simulation test results of the proposed control system were presented in figure 7.

Depicted in figure 7.A the angular velocity step responses of the control system show, that by using state feedback controller with load torque feedforward path, improvement of the dynamics could be achieved during the transient caused by the

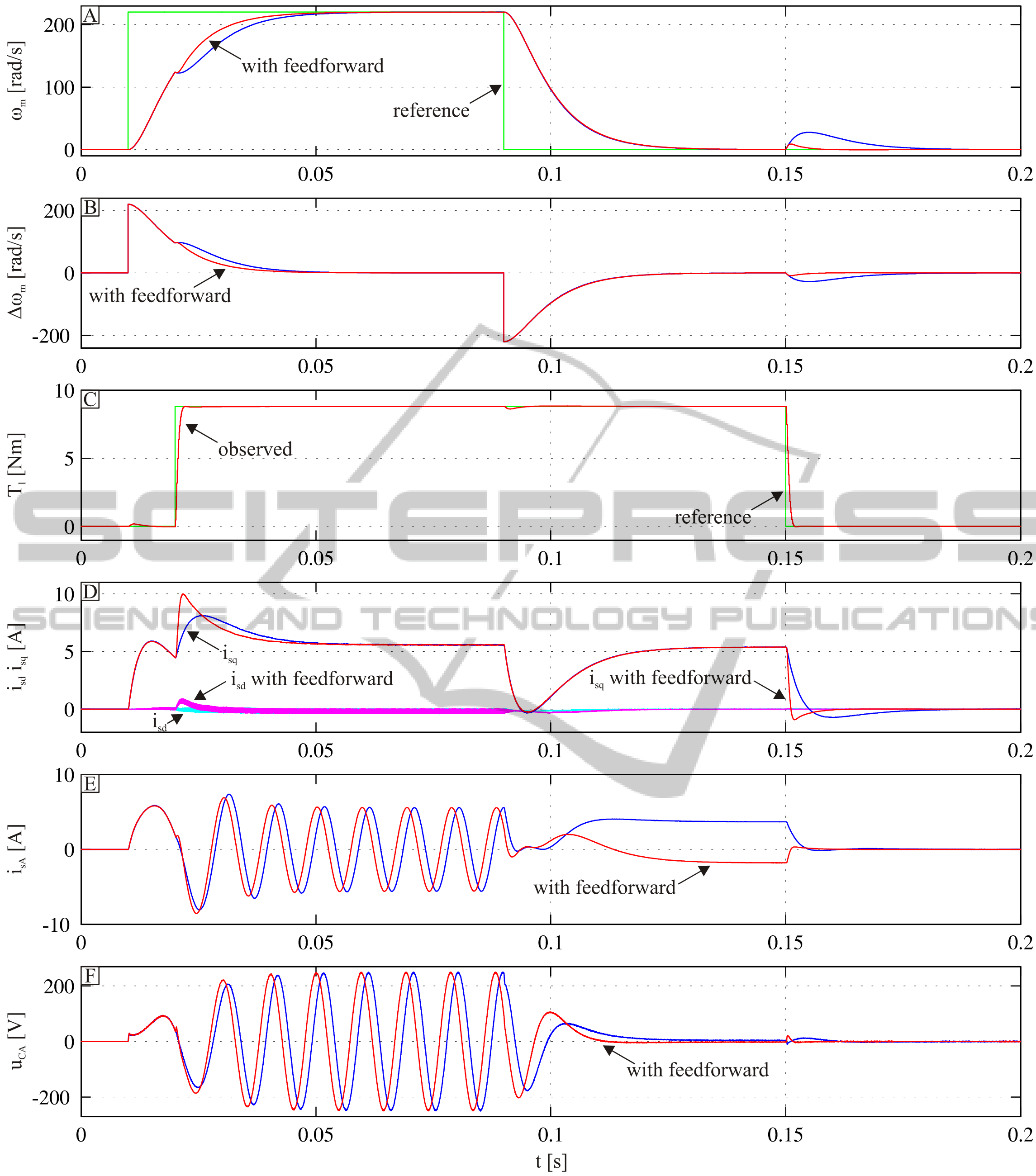

Figure 7: Simulation test results.

load torque step change. It can be seen, that the angular velocity error caused by load torque step changes at t = 20 ms and at t = 150 ms is smaller, when feedforward path is used. The use of the load torque feedforward path minimise the dynamic error by the transient.

The proper operation of the load torque observer is presented in figure 7.C. An actual value of the load torque is estimated with good dynamics and without steady state error.

It can be seen from figure 7.D, that the q-axis component of the current space vector is responsible for producing electromagnetic torque. PMSM operates with control strategy based on zero d-axis component of the current space vector.

By using of the LC filter, sinusoidal waveform of the input motor voltage can be obtained (figure 7.E). In this case, electromagnetic torque ripple reduction can be achieved.

7 CONCLUSIONS

This paper presents discrete full state feedback non-stationary controller with neural network based non-stationary load torque feedforward path. A mathematical formula how to calculate an appropriate non-stationary gain values for a feedforward was presented.

Designed neural network approximator was successfully implemented in a control system with PMSM fed by 3-level NPC inverter with output LC filter. The observed load torque has been used as an input signal for the feedforward path. Proposed feedforward path significantly improves dynamic properties of the considered control system during load torque changing.

Non-stationary discrete state feedback controller was designed in order to control the angular velocity of the PMSM and to provide control strategy based on zero *d*-axis component of the current space vector as well as sinusoidal waveforms of the input motor voltages.

The proposed control algorithm was successfully tested in a Matlab environment. Experimental verification of the designed control algorithm with NN feedforward path is planned in the future.

ACKNOWLEDGEMENTS

Research work financed by The National Science Centre (Poland) under Grant no 6636/B/T02/2011/40 (from 2011 to 2013).

REFERENCES

Huang, S., Tan, K. K., 2012. Intelligent Friction Modeling and Compensation Using Neural Network Approximations. *IEEE Transactions on Industrial Electronics*, vol. 59, no. 8, pp. 3342-3349.

Iwasaki, M., Seki, K., Maeda, Y., 2012. High-Precision Motion Control Techniques: A Promising Approach to Improving Motion Performance. *IEEE Industrial Electronics Magazine*, vol. 6, no. 1, pp. 32-40.

Lee, D.-C., Sul, S.-K., Park, M.-H., 1994. High performance current regulator for a field-oriented controlled induction motor drive. *IEEE Transactions on Industry Applications*, vol. 30 no. 5, pp. 1247-57.

Luenberger, D., 1971, An introduction to observers. *IEEE Transactions on Automatic Control*, vol. 16 no. 6, pp. 596-602.

Mun-Soo, K., Song, D.-S., Lee, Y.-K., Won, T.-H., Park, H.-W., Jung, Y.-I., Lee, M.H., Lee, H., 2001. A robust control of permanent magnet synchronous motor using load torque estimation. In *ISIE 2001*, *International Symposium on Industrial Electronics*, vol. 2, pp. 1157-1162.

Pajchrowski, T., Zawirski, K., 2012. Adaptive neural speed controller for PMSM servodrive with variable parameters. In *EPE/PEMC 2012*, *15th International Power Electronics and Motion Control Conference*, pp. LS6b.3-1-LS6b.3-5.

Pawlikowski, A., Grzesiak, L., 2007. Vector-Controlled Three-Phase Voltage Source Inverter Producing a Sinusoidal Voltage for AC Motor Drives. In *EUROCON 2007, The International Conference on "Computer as a Tool"*, pp. 1902-1909.

Pillay, P., Krishnan, R., 1988. Modeling of permanent magnet motor drives. *IEEE Transactions on Industrial Electronics*, vol. 35 no. 4, pp. 537-41.

Rodriguez, J., Bernet, S., Steimer, P.K., Lizama, I.E., 2010. A survey on Neutral-Point-Clamped inverters. *IEEE Transactions on Industrial Electronics*, vol. 57, no. 7, pp. 2219-2230.

Selmic, R. R., Lewis, F.L., 2000. Deadzone compensation in motion control systems using neural networks. *IEEE Transactions on Automatic Control*, vol. 45, no. 4, pp. 602-613.

Steinke, J. K., 1999. Use of an LC filter to achieve a motor-friendly performance of the PWM voltage source inverter. *IEEE Transactions of Energy Conversion*, vol. 14, no. 3, pp. 649-654.

Grzesiak, L. M., Tarczewski T., 2013. PMSM servo-drive control system with a state feedback and a load torque feedforward compensation, *COMPEL: The International Journal for Computation and Mathematics in Electrical and Electronic Engineering,* vol. 32 iss: 1, pp. 364-382.

Tarczewski, T., Grzesiak, L. M., 2012. State feedback control of the PMSM servo-drive with sinusoidal voltage source inverter. Power Electronics and Motion In *EPE/PEMC 2012*, *15th International Power Electronics and Motion Control Conference*, pp. DS2a.6-1-DS2a.6-6.

Tewari, A., 2002, *Modern Control Design*. Wiley, Chichester.

Zawirski, K., 2005. *Control of permanent magnet synchronous motor*, Poznan University of Technology Publishers.